

Permian exhumation of the Buffalo Pitts orogenic peridotite massif, northern Cordillera, Yukon

S.T. Johnston, D. Canil, and L.H. Heaman

Abstract: We report the results of a geochemical and U–Pb zircon geochronological study aimed at constraining the timing and tectonic setting of the exhumation of an orogenic peridotitic mantle massif in central Yukon within northern Canadian Cordillera. The Buffalo Pitts orogenic massif is inferred to have been exhumed into continental metasedimentary rocks within the pericratonic Yukon–Tanana terrane. Structurally admixed with the peridotite were boudins of metaleucogabbro and metatroctolite. A metamorphic aureole, defined by migmatite with abundant leucosome, characterizes the metasedimentary wall rocks to the massif. Whole-rock chemical analyses indicate significant light rare-earth element enrichment of the leucogabbro and the metatroctolite, characteristics commonly ascribed to within-plate or rift settings. Crystallization of the leucogabbro occurred at 261.5 ± 2.3 Ma. The metatroctolite yields a similar crystallization age. These ages are coeval with metamorphism of the wall rocks to the orogenic massif, as indicated by leucosome crystallization at 262.3 ± 0.43 Ma. These geochemical and geochronological data are consistent with the orogenic massif having been exhumed within a continental rift at about 262 Ma, giving rise to metamorphism of the upper crustal rocks into which the massif was exhumed, and coeval with rift-related magmatism. Regional considerations suggest that rifting occurred within the back arc of a northeast-facing magmatic arc, represented by the Klondike schist. Coeval eclogite and blueschist along the northeast margin of the Yukon–Tanana terrane may mark the paleo-trench, along which a southwest-dipping slab is assumed to have subducted beneath Yukon–Tanana terrane.

Résumé : Nous présentons les résultats d'une étude géochimique et géochronologique U–Pb sur zircons dont le but était de préciser le moment et l'environnement tectonique de l'exhumation d'un massif orogénique de péridotite du manteau dans le centre du Yukon à l'intérieur de la Cordillère canadienne. Le massif orogénique de Buffalo Pitts aurait été exhumé pour se retrouver dans des roches métasédimentaires à l'intérieur du terrane péricratonique de Yukon–Tanana. Des boudins de métaleucogabbro et de métatroctolite sont mélangés à la structure de la péridotite. Une auréole métamorphique, caractérisée par une migmatite avec d'abondants leucosomes, caractérise les épentes de roches métasédimentaires du massif. Des analyses chimiques sur la roche entière indiquent un enrichissement important en terres rares légères du leucogabbro et de la métatroctolite, des caractéristiques habituellement assignées à des environnements de plaques ou de distension. La cristallisation du leucogabbro s'est effectuée vers $261,5 \pm 2,3$ Ma et la métatroctolite a donné un âge de cristallisation semblable. Ces âges sont contemporains avec le métamorphisme des roches des épentes du massif orogénique, tel qu'indiqué par la cristallisation des leucosomes vers $262,3 \pm 0,43$ Ma. Ces données géochimiques et géochronologiques concordent avec les interprétations selon lesquelles le massif orogénique aurait été exhumé durant une distension continentale vers 262 Ma et qu'il est contemporain d'un magmatisme associé à la distension. Selon des considérations régionales, la distension se serait produite dans l'arrière-arc d'un arc magmatique exposé au nord-est et représenté par le schiste Klondike. Une éclogite et un schiste bleu contemporains situés le long de la bordure nord-est du terrane de Yukon–Tanana pourraient marquer la paléotranchée le long de laquelle une dalle à pendage sud-ouest aurait glissé par subduction sous le terrane de Yukon–Tanana.

[Traduit par la Rédaction]

Introduction

A large region of polydeformed, Paleozoic continental metasedimentary and metavolcanic rocks in the northern Cordillera is commonly referred to as the Yukon–Tanana

terrane (Mortensen 1992). The origin of this vast and structurally complicated pericratonic terrane remains enigmatic (Tempelman-Kluit 1976; Dusel-Bacon et al. 2002). The pericratonic character of much of the terrane, together with voluminous Devonian to Permian igneous rocks, implies that

Received 14 September 2005. Accepted 6 July 2006. Published on the NRC Research Press Web site at <http://cjcs.nrc.ca> on 19 April 2007.

Paper handled by Associate Editor W.J. Davis.

S.T. Johnston.¹ School of Earth and Ocean Sciences, University of Victoria, P.O. Box 3055 STN CSC, Victoria, BC V8W 3P6, Canada.

D. Canil. School of Earth and Ocean Sciences, University of Victoria, P.O. Box 3055 STN CSC, Victoria, BC V8W 3P6, Canada.

L.H. Heaman. Department of Earth and Atmospheric Sciences, University of Alberta, Edmonton, AB T6G 2E3, Canada.

¹Corresponding author (e-mail: stj@uvic.ca).

it originated in the Paleozoic as part of the North American passive margin, and that subsequently it was the site of a long-lived Andean-style arc (Mortensen 1992; Dusel-Bacon and Cooper 1999; Dusel-Bacon et al. 2002). Alternatively, based on correlations with similar pericratonic terranes in Alaska, the Yukon–Tanana terrane has been interpreted as a component of an exotic ribbon continent that collided and buckled forming a series of oroclinal folds along the western edge of the North American continent (Johnston 2001). Mesozoic and Cenozoic arcs constructed atop and tectonically emplaced onto this pericratonic continental substrate have further obscured its pre-Mesozoic history.

We recently documented the geological setting, geochemistry, and petrology of a orogenic peridotite massif and its continental metasedimentary wall rocks within the Yukon–Tanana terrane in central Yukon (Canil et al. 2003a). This peridotite massif was interpreted as a fragment of subcontinental mantle lithosphere exhumed during rifting of continental crust. Exhumation of hot mantle lithosphere into the continental crust caused heating and partial melting of pelitic rocks in an aureole surrounding the peridotite. Similar examples of mantle peridotite emplacement are well documented in the Ronda and other classic orogenic mantle massifs in the Alpine, Betic-Rif, and Pyrenean orogens (Platt and Vissers 1989; Muntener et al. 2000) but were hitherto unrecognized in the Cordillera of western North America.

Based on geological relationships in the country rocks and limited constraints from Os isotopes on the peridotite body, we suggested that mantle exhumation probably occurred in the Devonian. More precise constraints on the age and tectonic setting of this exhumation event are, however, important for establishing its relationship and broader significance in the evolution of Cordilleran continental crust. To this end, we present whole-rock geochemical and U–Pb geochronological data for key rocks in the aureole and in boudins structurally imbricated with the peridotite massif. These new data allow us to further refine suggested relationships among structurally admixed mantle peridotite, leucogabbro, leucosome, and troctolite; constrain the tectonic setting in which mantle exhumation and related magmatism and metamorphism occurred; and limit the timing and sequence of geologic events during mantle exhumation. Importantly, it appears that exhumation occurred much later—in the Permian—than we originally envisaged. In light of these constraints, we discuss the implications of mantle exhumation for the evolution of continental lithosphere in the northern portion of the Cordilleran orogen.

Geological setting

The Buffalo Pitts peridotite massif is situated northwest of Whitehorse, Yukon, near Mt. Pitts and Mt. Buffalo in the central Dawson Range, an area underlain by rocks of the Yukon–Tanana terrane (Fig. 1). The pericratonic Yukon–Tanana terrane includes an assemblage of metaquartzites and metapelites (Fig. 2) interpreted to have originated as sediments derived from erosion of a mid-Paleozoic calc-alkaline arc terrane that shed juvenile, mafic to intermediate detritus, and a Proterozoic and older craton, probably the Canadian Shield (Selby et al. 1999). Orthogneiss and amphibolite provide a record of the coeval Andean arc (Fig. 2). Regional lower amphibolite-facies metamorphism is suggested by the

presence of biotite and muscovite, with minor garnet in the metasedimentary rocks, and blue-green hornblende with minor garnet and diopside in amphibolite layers (Johnston and Hachey 1993; Evers et al. 2001). Layering and metamorphic minerals in the metamorphic rocks are cut by and predate mid-Cretaceous plutons and Early Jurassic dykes, limiting metamorphism to pre-Jurassic (Johnston 1999). Highly strained and recrystallized mid-Permian intrusions that form foliaform augen gneiss bodies provide an upper limit on the age of regional deformation and coeval metamorphism (Ryan et al. 2003b). The growth of metamorphic zircon during deformation of the Permian intrusions points to a Permian age for metamorphism (Ryan et al. 2003a). To the south of the study area, Early Jurassic plutons were synkinematic with regional, ductile deformation (Johnston and Erdmer 1995) implying that at least locally, the main fabric may be in part Early Jurassic.

The Buffalo Pitts peridotite is partially serpentinized and occurs within an areally extensive unit of graphitic quartzite and minor psammite and metapelite. Schistosity parallel to compositional layering within the metasedimentary unit strikes west to northwest and dips homoclinally north to northeast (Fig. 2). The peridotite occurs as a foliaform megaboudin or structural lens at least 500 m long enclosed within the metasedimentary rocks (Figs. 2, 3). Contacts between the peridotite and its host rocks are ductile shear zones. The shear zones consist largely of sheared metasedimentary rocks and are characterized by a significant reduction in grain size, the presence of intrafolial folds, and anastomosing high-strain zones. The regionally developed layering predates and appears drawn into and deformed within these ductile shear zones. A weakly developed compositional banding present within the peridotite parallels the contact. Metre-scale structural interleaving, with slices of peridotite and its host rocks imbricated along ductile shear zones, is common within the contact (Evers et al. 2001).

The peridotite massif lacks associated ophiolitic rocks (cumulates, sheeted dykes, pillow lavas, or abyssal sedimentary rocks) (Fig. 2), although as a structural lens, it is possible that structural dismemberment explains the isolation of the peridotite. Regional mapping (Ryan et al. 2003b) has demonstrated that amphibolites within the wall rocks are the metamorphosed equivalents of volcanic rocks that occur stratigraphically interlayered with and above the quartzose metasedimentary sequence. These metavolcanic rocks have been interpreted as part of a Devonian–Mississippian magmatic arc (Ryan et al. 2003b). In addition, a limited level of depletion in the peridotite (>3 wt.% Al_2O_3) is typical of mantle exposed in continental arcs, continental rifts, and as orogenic massifs, and unlike ophiolite mantle, which is usually more depleted (<2 wt.% Al_2O_3) (Canil et al. 2003b). The lack of any associated ophiolitic rocks and the limited level of depletion is consistent with interpretation of the peridotite body as an “orogenic type” or continental mantle peridotite (Den Tex 1969).

Elsewhere in Yukon–Tanana terrane, similar ultramafic bodies that lack associated ophiolitic strata have been interpreted as intrusions (Piercey and Murphy 2000; Ryan et al. 2003b; Piercey et al. 2004). An intrusive origin for the Buffalo Pitts peridotite can, however, be ruled out on the basis of a number of observations: (1) the presence of a solid-state,

Fig. 1. Regional geological map showing the distribution of the pericratonic Yukon–Tanana terrane (YTT) (Wheeler and McFeeley 1991), and location of study area just north of Mt. Pitts (BP, Buffalo Pitts peridotite) (after Canil et al. 2003a). Also shown for reference are the Stewart River (SR) region, the Permian Klondike schist, and regions characterized by blueschist and eclogite.

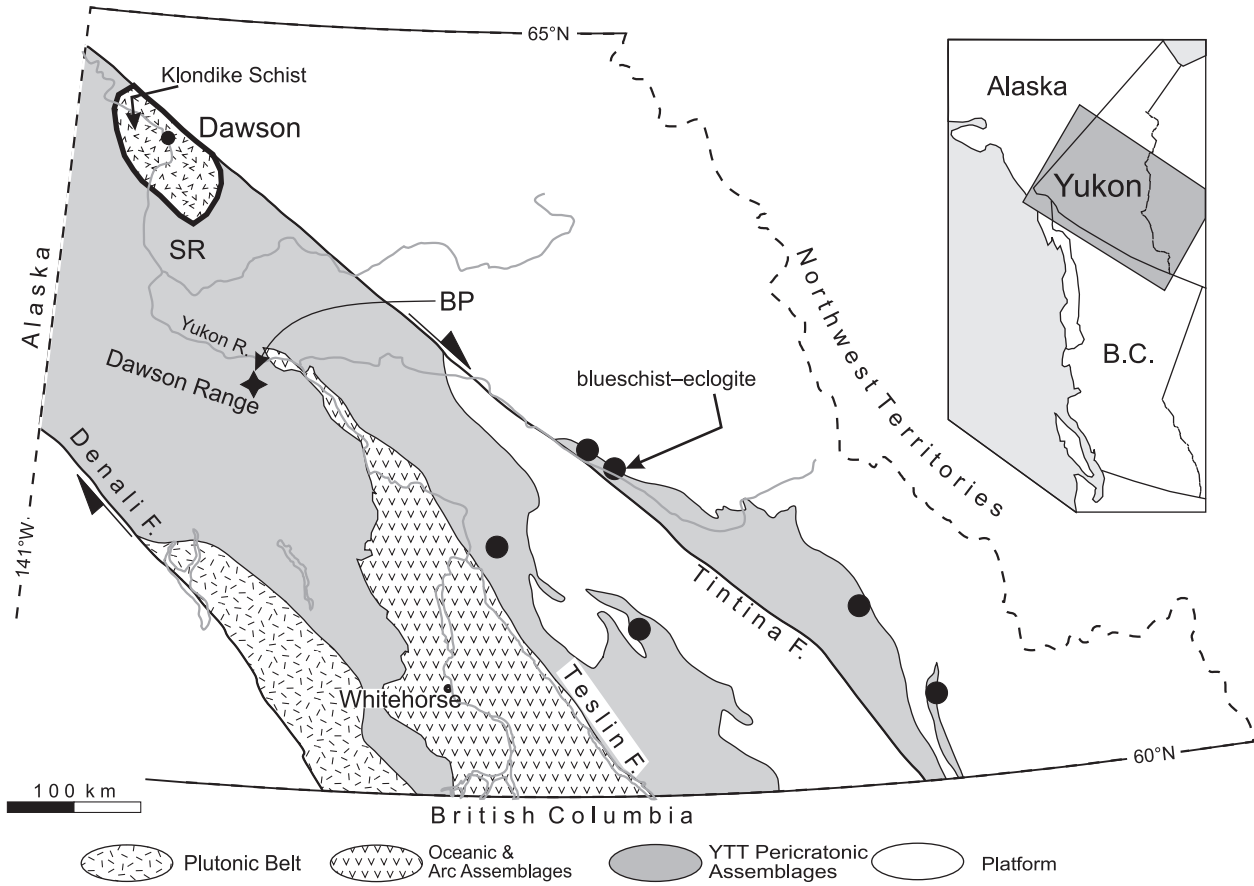


Fig. 2. Geology in the vicinity of the Buffalo Pitts peridotite. 1, Paleozoic (Devonian–Mississippian?) quartz–mica schist, carbonaceous quartzite and mica schist, and rare marble; 2, Devonian–Mississippian amphibolite and hornblende metabasite; 3, Mississippian hornblende and biotite–hornblende–quartz diorite, quartz monzonite, and granodiorite orthogneiss, regionally referred to as the Selwyn Gneiss; 4, Early Jurassic biotite hornblende granodiorite; 5, the Buffalo Pitts peridotite massif; 6, strike and dip of foliation. Interval of topographic contours is 500 feet (~152 m). Geology after Johnston and Hachey (1993), Johnston (1999), and unpublished data from S. Johnston (2000).

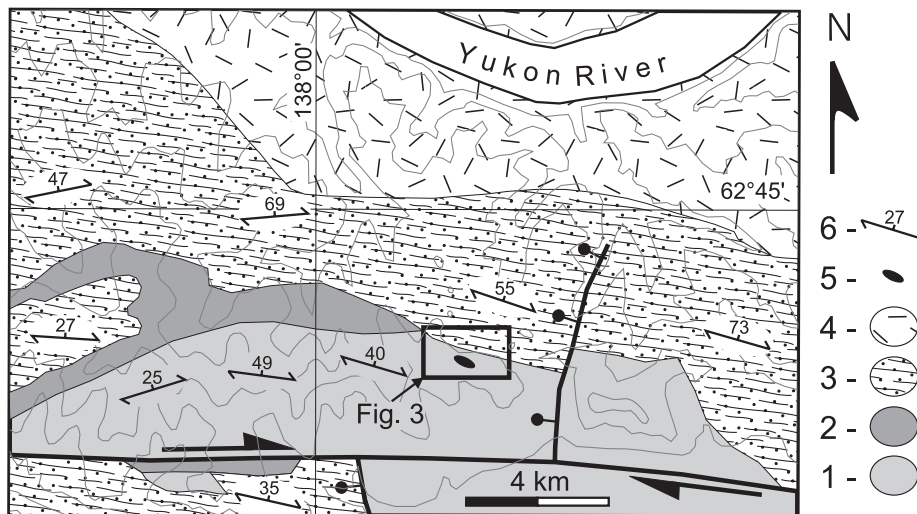
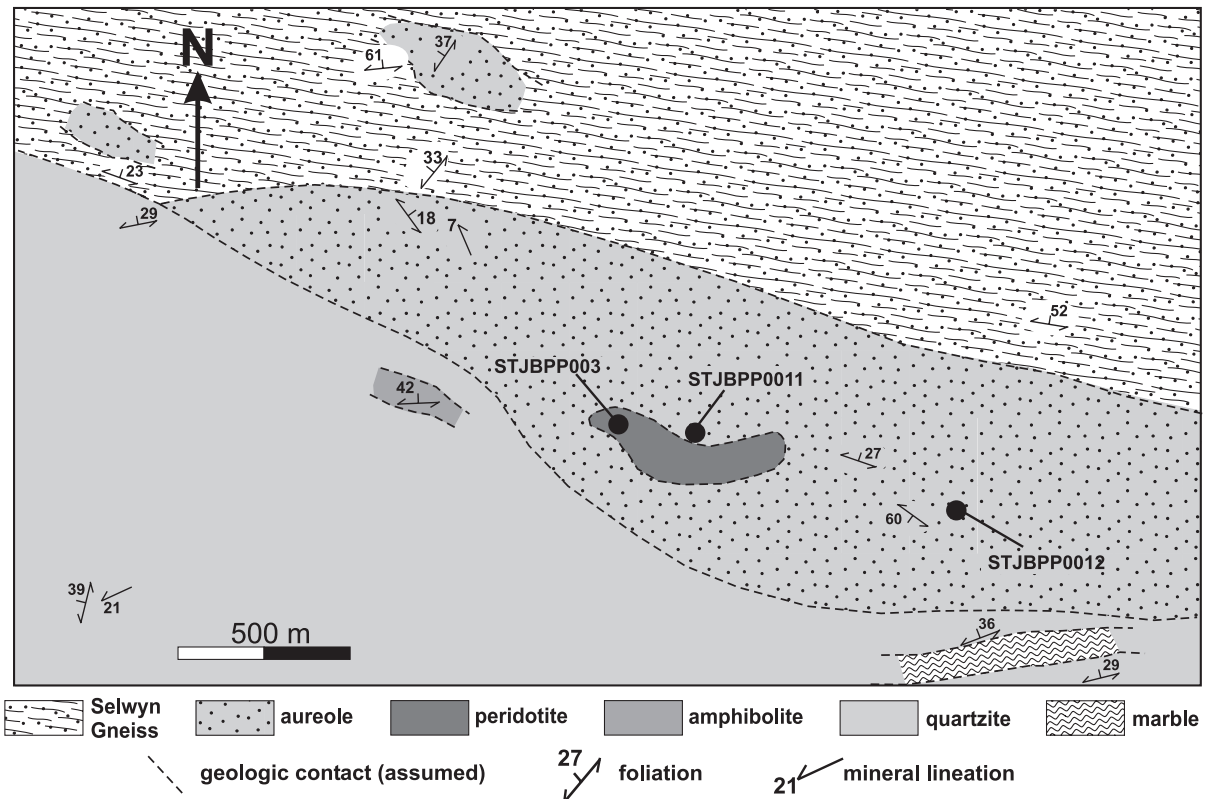


Fig. 3. Geology of the field area showing the orogenic peridotite massif and its aureole in Paleozoic metasedimentary country rocks (after Canil et al. 2003a). Figure location provided in Fig. 2. Sample locations with analytical data discussed in this paper are labelled.



protogranular and porphyroclastic layered metamorphic fabric, indicative of a high-temperature mantle deformation; (2) spinel grains exhibit holly-leaf crystal form characteristic of mantle conditions (not euhedral cubes); (3) the high-Al, low-Cr/Al character of the spinels (unlike the Cr-rich spinels of layered ultramafic intrusions); (4) plagioclase coronae on the holly-leaf spinel grains (the holly-leaf texture is indicative of mantle restites, and the plagioclase coronae record decompression from mantle pressures); and (5) the presence of stable co-existing Ol–Opx–Cpx–Sp–Phl (intrusions lack coexisting Sp–Opx–Cpx–Phl and are typically characterized by cumulus plagioclase).

A discordant boudin (1 m in diameter) of locally gneissic pegmatoid leucogabbro, bounded by ductile shear zones, occurs in the western portion of the peridotite body. The coarse grain size and lack of change in grain size toward the margins of this small body are consistent with interpreting the metaleucogabbro as a boudin or block structurally admixed with the peridotite body. The original relationship between the metaleucogabbro and the peridotite is unknown.

Immediately adjacent to the peridotite body are blocks of skarn and boudins of fine-grained metatroctolite with two-pyroxene coronae developed between olivine and plagioclase. Because the metatroctolite occurs as structural lenses and boudins, the original relationship to the peridotite remains unknown. The fine grain size of these metre-sized bodies indicates rapid cooling of the original intrusion, consistent with the troctolite originating as chilled dykes or sills. Growth of the two-pyroxene coronae between and at the expense of olivine and plagioclase requires pressures of 0.8 GPa and

indicates that corona development occurred at deep levels (>20 km) in the lower crust (Canil et al. 2003a). These relationships lead us to interpret the troctolites as having been dykes or sills that intruded into and cooled within the deep crust. We cannot, however, rule out the possibility that the troctolite boudins originated within shallow intrusions that were subsequently buried to lower crustal conditions.

The peridotite massif is surrounded by an aureole of blue quartzite with discontinuous and heterogeneous patches of leucosome developed in more pelitic layers (Fig. 3). The blue colour in the quartzite is imparted by its high apatite content (~5%) and minor blue corundum. It is unclear whether the high phosphorus (P) content is a primary feature of the quartzite or is the result of metasomatism, perhaps by light rare-earth element (LREE) enriched fluids fluxed through the crust during peridotite exhumation. The pressure–temperature (*P–T*) history of the peridotite and its country rocks was documented by Canil et al. (2003a). The metapelite leucosome in the country rock aureole shows biotite replaced by orthopyroxene, garnet, and sillimanite, and small Ca-rich garnet cores overgrown by euhedral Mg-rich garnet rims. Garnet–orthopyroxene Fe–Mg geothermometry requires prograde heating through a temperature of ~850 °C. In contrast to pelitic rocks in the aureole, the two-pyroxene geothermometry of the peridotite massif and troctolite boudins suggest cooling through 850 °C and ~0.7 GPa. Olivine–spinel Fe–Mg geothermometry in the peridotite is also consistent with cooling from 900 to ~600 °C.

The metasedimentary package hosting the Buffalo Pitts massif was intruded by arc-related granitoids at ~360 to

345 Ma (Mortensen 1992; Johnston 1995) and again in the mid-Permian (Mortensen 1990; Ryan et al. 2003b). The Selwyn Gneiss, a sheared body of coarse-grained, leucocratic, hornblende–biotite–quartz diorite to granodiorite, crops out north and structurally above the northeast-dipping rocks of the study area (Figs. 2, 3). The gneiss intrudes the meta-sedimentary package—quartz diorite dykes extend from the main body of the intrusion into the underlying metasedimentary rocks. Similar dykes intrude the peridotite massif. The gneiss body was previously assumed to be a Mississippian intrusion, based on a U–Pb zircon age determination of $355.4^{+13.7}_{-6.1}$ Ma for a sample of orthogneiss collected along the Yukon River, some 35 km along strike to the northwest from the study area (Mortensen 1986, 1992). The Selwyn Gneiss is intruded to the northeast by Early Jurassic granodiorite (Johnston and Hachey 1993).

Samples and methods

Three samples were selected for a geochronology study to constrain the age of exhumation and high-grade metamorphism. Petrographic descriptions of these rocks are given in Appendix A. The samples were processed at the University of Alberta, and processing followed the U–Pb geochronology procedures outlined by Heaman et al. (2002). Zircon fractions were recovered from samples of leucogabbro, troctolite boudin, and aureole leucosome. In each sample, two populations could be identified: (1) colourless to tan shards and fragments, and (2) subordinate number of colourless, resorbed, subhedral prismatic crystals (possibly xenocrysts). Many of the zircon fragments are Fe-stained and mineral inclusions are common. In addition to a moderate number of colourless irregular fragments of zircon, the troctolite sample contained a small amount of tiny brown, slightly resorbed baddelyite blades and some large tan titanite crystals with abundant oxide inclusions. None of these samples yielded zircon crystals that have an equant multifaceted morphology typical of zircon crystallizing during high-grade metamorphism of a mafic lithology (Creaser et al. 1997).

We determined the whole-rock geochemistry on two of the aforementioned samples: leucogabbro (STJBPP003) and the two-pyroxene corona troctolite (STJBPP0012). Centimetre-thick slabs of leucogabbro were cut, crushed in a jaw crusher, and reduced to a powder in a hardened steel ring mill. Major elements were determined by X-ray fluorescence (XRF) on glass disks and powder pellets at Global Discovery Labs, a subsidiary of Teck-Cominco, Vancouver, British Columbia. Trace elements were determined by solution nebulization inductively coupled plasma – mass spectrometry (ICP–MS) at the University of Victoria on rock powders dissolved in HF–HNO₃ following methods given in Canil et al. (2003a).

The troctolite boudins were typically <10 cm in diameter, limiting the amount of sample available for whole-rock analysis. Small slabs (~5 g) of this rock were cut, crushed, powdered, fused in a Pt crucible in air at 1500 °C for 48 h and quenched to a glass. Chips of the glass were mounted in epoxy and polished. Electron microprobe (EMP) and laser ablation ICP–MS were used to determine major and trace elements, respectively, in the glass chips. Analytical methods and conditions are described in Chen et al. (2000). Accuracies for

EMP are better than 1% for major elements and better than 10% for trace elements by LA (laser-ablation microprobe)–ICP–MS as determined by tests on MPI DING glasses (Canil et al. 2003b).

Results

Geochronology

U–Pb data from the analysis of 11 small, multigrain zircon analyses (7–50 fragments) from the three investigated samples are presented in Table 1 and Fig. 4. In addition, a multigrain fraction of colourless wedge-shaped crystals interpreted to be titanite was analyzed from leucosome sample STJBPP0011 (fraction 2). The zircon fractions have variable U contents (15–533 ppm) but generally have high Th/U (0.31–0.83), consistent with an igneous origin. The majority of the zircon analyses are concordant with ²⁰⁶Pb/²³⁸U dates that vary within the narrow range between 268 and 257 Ma (excluding metatroctolite analysis #1), indicating that the majority of zircon growth in these three samples is of Permian age.

The geochemistry of all three zircon fractions from leucogabbro sample STJBPP003 is similar (moderate U content and high Th/U) but there is some variation in the ²⁰⁷Pb/²⁰⁶Pb dates (263–254 Ma). Fraction 1 is the least precise of the three and is characterized by significant common Pb (31 pg versus 12 and 13 pg of total common Pb, and ²⁰⁶Pb/²⁰⁴Pb ratios of 1713 versus 7179 and 4047 for fractions 2 and 3, respectively). The two most precise analyses (#2 and #3) have similar ²⁰⁷Pb/²⁰⁶Pb dates of 262.6 and 260.4 Ma, respectively. Because of the large common Pb correction required for fraction 1, we discard it and interpret the average ²⁰⁷Pb/²⁰⁶Pb age of fractions 2 and 3 (261.5 ± 2.3 Ma) as the best estimate for the time of zircon growth in this sample (Fig. 4a).

Four zircon fractions analyzed from leucosome sample STJBPP0011 (Fig. 4b) range from –0.3% to 17.2% discordant. The discordance is reflected in the ²⁰⁷Pb/²⁰⁶Pb ages, which range from 315 to 257 Ma. Fraction 3, although concordant, shows a large uncertainty reflecting the very small amount of Pb (100 pg total), and the resulting age estimate is highly sensitive to the applied blank and common Pb corrections. The two most precise analyses (#1 and #5) yield almost identical ²⁰⁶Pb/²³⁸U dates of 262.4 and 262.3 Ma, respectively. A weighted average ²⁰⁶Pb/²³⁸U date of fractions 1, 5, and 4 (which, although characterized by minor inheritance, yielded a similar ²⁰⁶Pb/²³⁸U age of 262.4 Ma) gives an age of 262.32 ± 0.43 Ma and is interpreted as the best estimate of the age of crystallization of the leucosome. This age overlaps in error with the age of the leucogabbro and indicates that magmatism and leucosome development were coeval. The one titanite fraction (#2) has very low U and Pb concentrations, is strongly discordant, and did not yield any useful information.

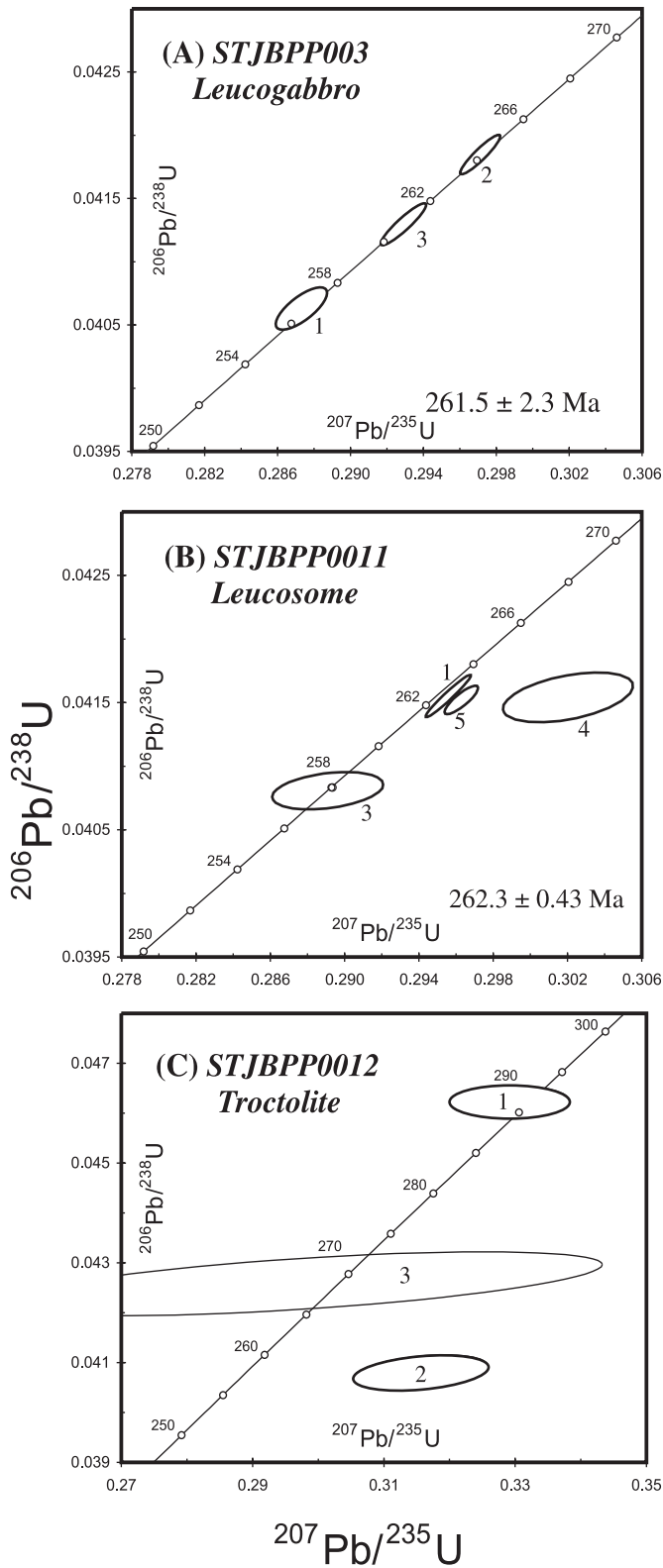
The U–Pb results for three multigrain zircon fractions for metatroctolite sample STJBPP0012 (Fig. 4c) are difficult to interpret, and a precise age determination is not possible. The ²⁰⁶Pb/²³⁸U dates vary between 291 and 258 Ma, and all three samples are characterized by low precision and variable (–19% to 44%) discordance. Two fractions (#1 and #2) have low Pb contents (200 and 30 pg, respectively). The ²⁰⁶Pb/²³⁸U age (268.8 ± 1.6 Ma) of fraction 3 is the most

Table 1. U–Pb results for samples associated with an orogenic peridotite massif in the Yukon–Tanana Terrane, northern Cordillera.

Description	Weight (μg)	U (ppm)	Th (ppm)	Pb (ppm)	Th/U	TCPb (pg)	Model Ages (Ma)							% Disc.
							$\frac{^{206}\text{Pb}}{^{204}\text{Pb}}$	$\frac{^{206}\text{Pb}}{^{238}\text{U}}$	$\frac{^{207}\text{Pb}}{^{235}\text{U}}$	$\frac{^{207}\text{Pb}}{^{206}\text{Pb}}$	$\frac{^{206}\text{Pb}}{^{238}\text{U}}$	$\frac{^{207}\text{Pb}}{^{235}\text{U}}$	$\frac{^{207}\text{Pb}}{^{206}\text{Pb}}$	
STJBPP003 Leucogabbro (0350150E, 6956946N)														
1 z, col shards 0NM (23)	60	338	251	16	0.74	31	1713	0.04063 \pm 7	0.2873 \pm 6	0.05129 \pm 7	256.8 \pm 0.4	256.5 \pm 0.5	253.7 \pm 3.0	–1.2
2 z, col shards 0NM (24)	90	350	268	16	0.77	12	7179	0.04185 \pm 6	0.2971 \pm 5	0.05149 \pm 3	264.3 \pm 0.4	264.1 \pm 0.4	262.6 \pm 1.2	–0.7
3 z, tan equant 0NM (8)	72	288	208	13	0.72	13	4047	0.04130 \pm 6	0.2929 \pm 5	0.05143 \pm 4	260.9 \pm 0.4	260.9 \pm 0.4	260.4 \pm 1.6	–0.2
STJBPP0011 Leucosome (0350356E, 6956904N)														
1 z, col shards 10NM (38)	82	344	229	16	0.67	10	7589	0.04155 \pm 7	0.2954 \pm 5	0.05157 \pm 2	262.4 \pm 0.4	262.8 \pm 0.4	266.5 \pm 0.9	1.6
2 t, col wedges 10NM (30)	75	0.09	0.07	0.09	0.83	8	23	0.1002 \pm 71	1.031 \pm 357	0.0747 \pm 252	615 \pm 41	720 \pm 166	1060 \pm 100	44.0
3 z, col frags 10NM (50)	101	23	12	1.1	0.52	10	633	0.04081 \pm 6	0.2890 \pm 12	0.05136 \pm 20	257.9 \pm 0.4	257.8 \pm 1.0	257.2 \pm 9.0	–0.3
4 z, col prisms and frags 10NM (10)	19	496	282	23.3	0.57	25	994	0.04154 \pm 8	0.3018 \pm 14	0.05269 \pm 22	262.4 \pm 0.5	267.8 \pm 1.1	315.6 \pm 9.5	17.2
5 z, col to lt yellow shards 10NM (18)	29	533	354	24.6	0.67	13	3193	0.04152 \pm 5	0.2961 \pm 4	0.05173 \pm 3	262.3 \pm 0.3	263.4 \pm 0.3	273.4 \pm 1.5	4.2
STJBPP0012 Metatroctolite (0351055E, 6956699N)														
1 z, col shards (30)	48	58	33	3.9	0.57	55	163	0.04623 \pm 13	0.3291 \pm 37	0.05163 \pm 59	291.3 \pm 0.8	288.9 \pm 2.8	269.2 \pm 25.9	–8.4
2 z, tan large frags (7)	41	15	4.8	0.8	0.31	5	326	0.04081 \pm 14	0.3156 \pm 42	0.05608 \pm 70	257.9 \pm 0.9	278.5 \pm 3.2	455.4 \pm 27.3	44.2
3 z, col tiny frags (45)	85	86	54	4.4	0.63	44	461	0.04258 \pm 26	0.2976 \pm 187	0.05069 \pm 300	268.8 \pm 1.6	264.5 \pm 14.5	227 \pm 100	–18.8

Note: 0NM refers to a nonmagnetic mineral fraction on a Frantz Isodynamic Separator with a 0 degree side tilt. 10NM is the nonmagnetic fraction at 10° tilt. TCPb, Total Common Pb. All errors in this table reported at 1 σ . Locations given in Universal Transverse Mercator (UTM) Easting and Northing for Zone 8. z, zircon; col, colourless; lt, light; frags, fragments; number in parentheses corresponds to the total number of grains analyzed; %Disc., discordance (in %).

Fig. 4. U–Pb concordia plots for samples in this study.



reliable estimate of the age of crystallization. Given these constraints, the best that can be said at present is that the troctolite is Middle Permian and possibly the same age as the leucogabbro and the leucosome.

Table 2. Whole-rock chemistry of Buffalo Pitts samples.

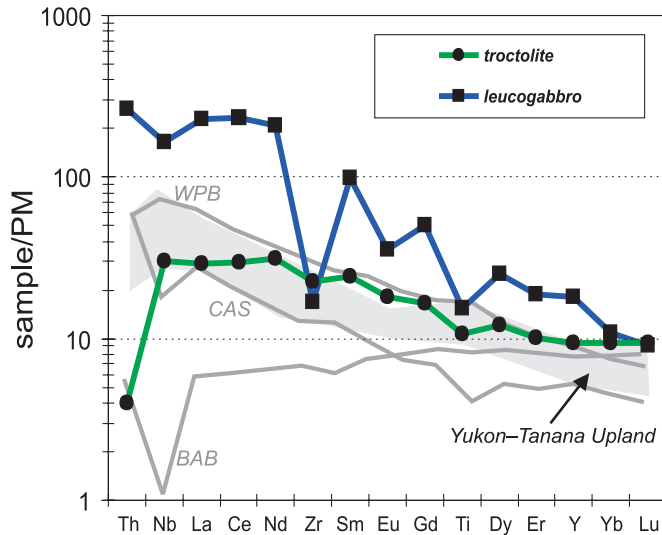
	STJBPP003	STJBPP0012
SiO ₂ (wt.%)	50.1	47.3
TiO ₂	3.31	1.76
Al ₂ O ₃	16.06	12
FeO	3.62	11.8
MnO	0.1	0.18
MgO	3.6	12.12
CaO	15.4	11.54
Na ₂ O	1.5	1.73
K ₂ O	1.2	0.5
P ₂ O ₅	1.49	
LOI	1.87	
Total	98.25	98.93
P (ppm)	5861	nd
Cr	40	nd
Co	32	nd
Ni	27	258
Sc	12.3	50.3
V	198	302
Rb	46.1	nd
Sr	724	149
Y	77.5	40.4
Zr	177.4	238.4
Nb	108.8	19.7
Ba	904	nd
La	148.42	18.78
Ce	392.28	49.37
Pr	53.53	8.07
Nd	260.53	39.11
Sm	40.11	9.77
Eu	5.44	2.78
Gd	27.40	8.93
Tb	3.39	1.41
Dy	17.04	8.19
Ho	2.94	1.58
Er	8.29	4.45
Tm	0.83	0.63
Yb	4.76	4.14
Lu	0.61	0.63
Th	21.23	0.32
U	4.58	0.11

Note: LOI, loss on ignition.

Whole-rock geochemistry

The small number of samples, together with the metamorphosed character of the rocks, limits the conclusions that can be drawn from our geochemical investigation. Recrystallization at amphibolite- to granulite-facies conditions implies that the major-element content (Table 2) may not be primary, and samples cannot be classified using conventional major-element schemes. Replacement of pyroxene by actinolite, and plagioclase

Fig. 5. Chemical data for immobile elements for troctolite and leucogabbro samples from this study normalized to primitive mantle (PM) (McDonough and Sun 1995). Typical patterns for within-plate (WPB), calc-alkaline arc (CAS), and back-arc basin (BAB) basalts are shown for reference as thick grey lines (Jenner et al. 1993). The grey shaded field encompasses all patterns of mid-Paleozoic amphibolites in the Lake George assemblage in the Yukon–Tanana Uplands (Dusel-Bacon and Cooper 1999).



clase by calcite (STJBPP003), further enforces the need for conservatism in interpretation of our data.

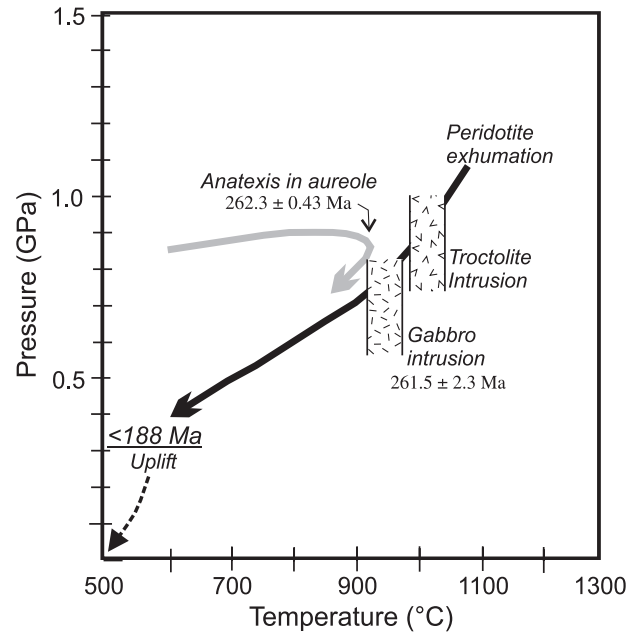
Patterns for trace elements known to be largely immobile during metamorphism show the troctolite boudin to be enriched in LREE, Zr, Nb, and Ti (Fig. 5). The leucogabbro has a high P and Ti content, explicable owing to extreme fractionation typically observed in pegmatoid gabbros and consistent with the abundant primary apatite and Fe–Ti oxide in the mode. The enrichment in P and Ti is further reflected by an extremely LREE-enriched pattern (nearly $200 \times$ primitive mantle) (Fig. 5).

Discussion

We identified and sampled boudins and tectonic lenses of granulite-facies leucogabbro, troctolite, and peridotite of the Buffalo Pitts mantle massif that are structurally admixed with a Devonian–Mississippian metasedimentary sequence. Because lenses of these rock types are unknown outside the mantle massif (Johnston 1995), we assumed that they were geologically related to one another and to the mantle peridotite. Our geochemical and geochronological data allow us to test this assumption.

Whole-rock geochemical analyses of the metatroctolite and the metaleucogabbro indicate that both rocks are characterized by LREE enrichment (extreme enrichment in the case of the leucogabbro) and elevated Ti (Fig. 5). The elevated Zr, Nb, and Ti concentrations in the troctolite, together with the observed LREE enrichment, are attributes commonly associated with mafic igneous rocks found within intraplate rift settings. Similarly, the extreme LREE enrichment and high P and Ti content of the leucogabbro are matched only by continental rift magmatic rocks, such as carbonatites, trachytes,

Fig. 6. Diagram summarizing the cooling and uplift history of samples from this study. The P – T – t paths are constrained by textural and thermobarometric constraints (Canil et al. 2003a). Solid black line shows the inferred P – T – t path of the peridotite mantle, the grey line of the crustal rocks entrained with the peridotite massif during exhumation. Post-188 Ma uplift (dashed black line) is inferred from published $^{40}\text{Ar}/^{39}\text{Ar}$ ages in hornblende and biotite (Dusel-Bacon et al. 2002; Villeneuve et al. 2003).

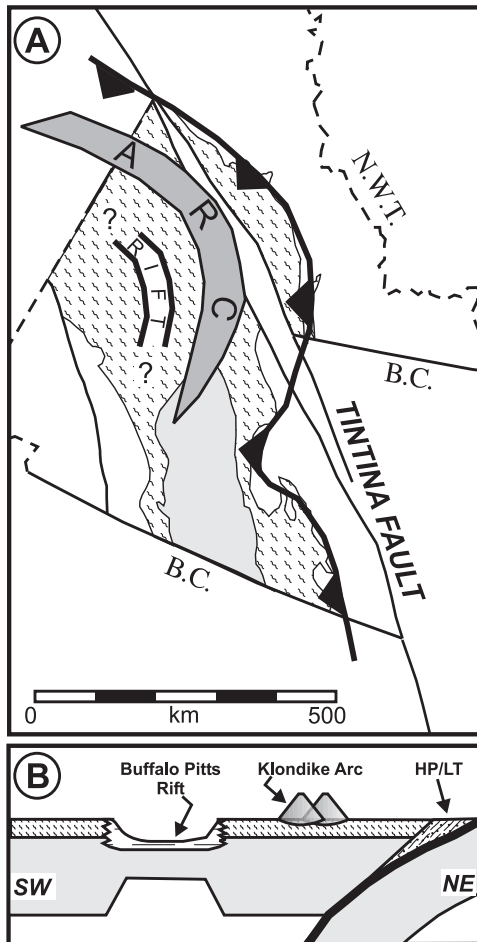


and phonolites. Our geochronological data confirm the temporal correlation of the troctolite and leucogabbro (Fig. 4) and allow us to establish the timing of the P – T – t (time) path of the mantle peridotite and entrained crustal rocks during exhumation (Fig. 6). Canil et al. (2003a), on the basis of mineral textures and mineral equilibria, established that the minimum pressure of origin of the mantle peridotite was at least 0.9 GPa. Metasedimentary rocks entrained with the peridotite during exhumation followed a clockwise P – T – t path during which they were contact metamorphosed and melted, giving rise to the 262 Ma leucosomes, at temperatures of 800 to 900°C and pressures of 0.7 to 0.8 GPa. Coeval decompressive, rift-related gabbroic and troctolitic magmatism corroborate the Middle Permian timing of rifting and mantle exhumation (Fig. 6).

The similarity of the Buffalo Pitts peridotite body and its host rocks, their textures, compositions, and P – T history with those from documented rifted continental settings in the Alps, Betic Rif, Red Sea, Pyrenees, and Iberia (Loomis 1972; Bonatti and Seyler 1987; Beslier et al. 1996; Muntener et al. 2000) argue for its exhumation within a rift setting. Together, the geological, geochemical, and geochronological data are consistent with exhumation of the peridotite and intrusion of the leucogabbro and the troctolite within a Permian rift setting. Therefore, the current spatial association of these rock suites is, despite their subsequent structural mixing and imbrication, likely the result of their original genetic association.

We had previously interpreted rifting and peridotite exhumation as having occurred in the Devonian. A Devonian age

Fig. 8. (A) Paleogeographic map of the northern Cordillera with 425 km of dextral displacement along the Eocene Tintina Fault restored, showing the distribution of Permian tectonic elements. The black line with teeth indicates the approximate location of the west-dipping subduction zone (constrained by the occurrence of blueschist and eclogite), the related magmatic arc (represented by metarhyolites of the Klondike Schist), and the back-arc rift in which the Buffalo Pitts orogenic massif was emplaced. (B) A schematic cross-section drawn from southwest to northeast showing the relationship of tectonic elements. HP/LT, high pressure and low temperature.



Yukon–Tanana terrane. Such a model might better explain the fact that almost all of the Klondike Schist has the bulk composition of rhyolite. A model of crustal melting is supported by evidence of a widespread elevated geothermal gradient as indicated by Permian igneous overgrowths on detrital zircons in metaconglomerate in the Stewart River area (Villeneuve et al. 2003).

At present, the Buffalo Pitts orogenic peridotite and its associated magmatic rocks are the only known manifestation of rifting within the back-arc region of the Andean Klondike Arc. Recent mapping along strike to the northwest in the Stewart River area has not revealed the presence of orogenic mantle massifs of the kind we describe. Bedrock in this part of Yukon is, however, poorly exposed. Even the body we describe is small, and it was previously unrecognized as an orogenic massif during mapping at 1 : 50 000 scale in this

heavily vegetated area (Johnston and Hachey 1993). Hundreds of other mantle tectonite occurrences are recognized along strike to the northwest in Yukon and Alaska (Foster et al. 1994; Ryan et al. 2003b). Many of these are klippen of ophiolite that, unlike the Buffalo Pitts body, are associated with weakly metamorphosed greenstones and chert and lack a penetrative tectonic fabric. Some, however, lack ophiolitic associations, and it seems likely that some of these may be additional orogenic massifs produced during rifting. Identification and study of these massifs are necessary to define the geometry and evolution of the Permian rift leading to exhumation of the Buffalo Pitts orogenic massif. The presence of Permian tuffs in the Nasina Series (Devonian and younger) confirms that quartzose clastic sedimentation occurred coeval with rifting. Mapping of the distribution and thickness of Permian sedimentary rocks may help further constrain the rift geometry and may aid in determining if rifting proceeded to a drift phase, with the production of oceanic crust. If drift did occur, it begs the question: what did the Yukon–Tanana terrane rift away from, and where is it now?

Conclusions

The new geochronological and geochemical data presented here allow us to conclude that (1) the exhumation of the Buffalo Pitts orogenic mantle massif within the pericratonic Yukon–Tanana terrane occurred in the Permian at about 262 Ma; (2) exhumation occurred within a rift setting, with coeval alkalic, within-plate, rift-related magmatism, represented by leucogabbro (261.5 ± 2.3 Ma) and metatroctolite boudins that are now found structurally admixed with the mantle massif; and (3) leucosome in the migmatized meta-sedimentary rocks that host the mantle massif crystallized at 262.3 ± 0.43 Ma, providing a record of synkinematic metamorphism of the upper crustal rocks, into which the mantle massif was exhumed. Rifting and mantle massif exhumation was coeval with high-*P* and low-*T* eclogitic and blueschist metamorphism along the northeastern limit of the Yukon–Tanana terrane and with felsic magmatism. The belt of felsic magmatic rocks, including the rhyolitic Klondike Schist, lay between the high-*P* and low-*T* metamorphic rocks to the northeast and the Buffalo Pitts region to the southwest. These relationships are best explained in terms of a model of southwest-dipping subduction along the northeastern margin of the Yukon–Tanana terrane, with the high-*P* and low-*T* metamorphic rocks marking the approximate location of the paleo-trench, and the felsic Klondike Schist representing the arc. In this model, the Buffalo Pitts orogenic massif is explained as a product of rifting within the back-arc region of the Klondike Arc. Rifting in and adjacent to the Klondike Arc may help explain its rhyolitic character.

Acknowledgments

We thank the field efforts and good cheer of K. Evers and K. Larson. W. Davis, C. Dusel-Bacon, J. Ryan, M. Colpron, M. Schmitz, and D. Murphy are thanked for journal reviews that significantly improved our manuscript. Editor Bill Davis provided excellent advice and guidance. This study was supported financially by Natural Sciences and Engineering Re-

search Council of Canada Discovery and Yukon Geology Program research grants to DC and STJ.

References

- Beslier, M.O., Cornen, G., and Girardeau, J. 1996. Tectono-metamorphic evolution of peridotites from the ocean/continent transition of the Iberia abyssal margin. *In* Proceedings Ocean Drilling Program, Scientific Results. Ocean Drilling Program, College Station, Tex., pp. 397–412.
- Bonatti, E., and Seyler, M. 1987. Crustal underplating and evolution of the Red Sea rift: Uplifted gabbro–gneiss crustal complexes on Zabargad and Brothers Islands. *Journal of Geophysical Research*, **92**: 12 803 – 12 821.
- Breitsprecher, K., and Mortensen, J.K. 2004. YukonAge 2004: a database of isotopic age determinations for rock units from Yukon Territory. *In* Canadian Geochronology Knowledgebase. Yukon Geological Survey, Whitehorse, Yukon. (CD-ROM.)
- Canil, D., Johnston, S.T., Evers, K., Shellnut, J.G., and Creaser, R.A. 2003a. Mantle exhumation in an early Paleozoic passive margin, northern Cordillera, Yukon. *Journal of Geology*, **111**: 313–327.
- Canil, D., Schulze, D.J., Hall, D., Hearn, B.C., Jr., and Milliken, S.M. 2003b. Lithospheric roots beneath western Laurentia: the geochemical signal in mantle garnets. *Canadian Journal of Earth Sciences*, **40**: 1027–1051.
- Chen, Z., Canil, D., and Longerich, H.P. 2000. Automated in-situ trace element analysis of silicate materials by laser ablation inductively coupled plasma mass spectrometry. *Fresenius' Journal of Analytical Chemistry*, **368**: 73–78.
- Colpron, M., and Group, Y.-T.W. 2001. Ancient Pacific Margin – an update on stratigraphic comparison of potential volcanogenic massive sulphide-hosting successions of Yukon–Tanana Terrane, northern British Columbia and Yukon. *In* Yukon exploration and geology 2000. Exploration and Geological Services Division, Yukon, Indian and Northern Affairs Canada, Whitehorse, Yukon, pp. 97–110.
- Creaser, R.A., Heaman, L.M., and Erdmer, P. 1997. Timing of high-pressure metamorphism in the Yukon–Tanana terrane, Canadian Cordillera: constraints from U–Pb zircon dating of eclogite from the Teslin tectonic zone. *Canadian Journal of Earth Sciences*, **34**: 709–715.
- Den Tex, E. 1969. Origin of ultramafic rocks, their tectonic setting and history: a contribution to the discussion of the paper “The origin of ultramafic and ultrabasic rocks” by P.J. Wyllie. *Tectonophysics*, **7**: 457–488.
- Dusel-Bacon, C., and Cooper, K.M. 1999. Trace-element geochemistry of metabasaltic rocks from the Yukon–Tanana Upland and implications for the origin of tectonic assemblages in east-central Alaska. *Canadian Journal of Earth Sciences*, **36**: 1671–1695.
- Dusel-Bacon, C., Lanphere, M.A., Sharp, W.D., Layer, P.W., and Hansen, V.L. 2002. Mesozoic thermal history and timing of structural events for the Yukon–Tanana Upland, east-central Alaska: $^{40}\text{Ar}/^{39}\text{Ar}$ data from metamorphic and plutonic rocks. *Canadian Journal of Earth Sciences*, **39**: 1013–1051.
- Erdmer, P. 1987. Blueschist and eclogite in mylonitic allochthons, Ross River and Watson Lake area, southeastern Yukon. *Canadian Journal of Earth Sciences*, **24**: 1439–1449.
- Erdmer, P., and Helmstaedt, H. 1983. Eclogite from central Yukon: a record of subduction at the western margin of ancient North America. *Canadian Journal of Earth Sciences*, **20**: 1389–1408.
- Erdmer, P., Ghent, E.D., Archibald, D.A., and Stout, M.Z. 1998. Paleozoic and Mesozoic high-pressure metamorphism at the margin of ancestral North America in central Yukon. *Geological Society of America Bulletin*, **110**: 615–629.
- Evers, K.G., Johnston, S.T., and Canil, D. 2001. An alpine peridotite in the Dawson Range, Yukon–Tanana terrane: preliminary results and interpretations. *In* Yukon exploration and geology 2000. Exploration and Geological Services Division, Yukon, Indian and Northern Affairs Canada, pp. 137–146.
- Foster, H.L., Keith, T.E.C., and Menzie, W.D. 1994. Geology of the Yukon–Tanana area of east-central Alaska. *In* The geology of Alaska. Edited by G. Plafker and H.C. Berg. The Geology of North America, Decade of North American Geology, Geological Society of America, Boulder, Colo., Vol. G-1, pp. 205–240.
- Heaman, L.M., Erdmer, P., and Owen, J.V. 2002. U–Pb geochronologic constraints on the crustal evolution of the Long Range Inlier, Newfoundland. *Canadian Journal of Earth Sciences*, **39**: 845–865.
- Jenner, G.A., Foley, S.F., Jackson, S.E., Green, T.H., Fryer, B.J., and Longerich, H.P. 1993. Determination of partition coefficients for trace elements in high-pressure temperature experimental run products by Laser Ablation Microprobe Inductively Coupled Plasma Mass Spectrometry (LAM–ICP–MS). *Geochimica et Cosmochimica Acta*, **57**(23–24): 5099–5103.
- Johnston, S.T. 1995. Geological compilation with interpretation from geophysical surveys of the northern Dawson Range, central Yukon (115 J/9 & 10; 115 I/12). *In* Open File 1995-2(G). Exploration and Geological Services Division, Yukon, Indian and Northern Affairs Canada, Whitehorse, Yukon, map scale 1 : 125 000.
- Johnston, S.T. 1999. Large scale coast-parallel displacements in the Cordillera: a granitic resolution to a paleomagnetic dilemma? *Journal of Structural Geology*, **21**: 1103–1108.
- Johnston, S.T. 2001. The Great Alaskan Terrane Wreck: Reconciliation of paleomagnetic and geological data in the northern Cordillera. *Earth and Planetary Science Letters*, **193**: 259–272.
- Johnston, S.T., and Erdmer, P. 1995. Magmatic flow and emplacement foliations in the Early Jurassic Aishihik Batholith, southwest Yukon: implications for northern Stikinia. *In* Jurassic magmatism and tectonics of the North American Cordillera. Geological Society of America, Denver, Colo., pp. 65–82.
- Johnston, S.T., and Hachey, N. 1993. Preliminary results of 1 : 50 000 scale geologic mapping in Wolverine Creek map area (115 I/12), Dawson range, southwest Yukon. Exploration and Geological Services Division, Yukon, Indian and Northern Affairs Canada, pp. 49–60.
- Johnston, S.T., Mortensen, J.K., and Erdmer, P. 1996. Igneous and meta-igneous age constraints for the Aishihik metamorphic suite, southwest Yukon. *Canadian Journal of Earth Sciences*, **33**: 1543–1555.
- Loomis, T.P. 1972. Contact metamorphism of pelitic rock by the Ronda ultramafic intrusion, southern Spain. *Geological Society of America Bulletin*, **83**: 2449–2474.
- McDonough, W.F., and Sun, S.S. 1995. The composition of the Earth. *Chemical Geology*, **120**: 223–253.
- Mohr, P. 1992. Nature of the crust beneath magmatically active continental rifts. *Tectonophysics*, **213**: 269–284.
- Mortensen, J.K. 1986. U–Pb ages for granitic orthogneiss from western Yukon Territory: Selwyn Gneiss and Fiftymile Batholith revisited. Geological Survey of Canada, Paper 86-1B, pp. 141–146.
- Mortensen, J.K. 1990. Geology and U–Pb geochronology of the Klondike District, west-central Yukon Territory. *Canadian Journal of Earth Sciences*, **27**: 903–914.
- Mortensen, J.K. 1992. Pre-mid-Mesozoic tectonic evolution of the Yukon–Tanana terrane, Yukon and Alaska. *Tectonics*, **11**(4): 836–853.

- Muntener, O., Hermann, J., and Trommsdorff, V. 2000. Cooling history and exhumation of lower-crustal granulite and upper mantle (Malenco, eastern central Alps). *Journal of Petrology*, **41**: 175–200.
- Piercey, S.J., and Murphy, D.C. 2000. Stratigraphy and regional implications of unstrained Devonian–Mississippian volcanic rocks in the Money Creek thrust sheet, Yukon–Tanana Terrane, southeastern Yukon. *In* Yukon exploration and geology 1999. Exploration and Geological Services Division, Yukon, Indian and Northern Affairs Canada, Whitehorse, Yukon, pp. 67–78.
- Piercey, S.J., Murphy, D.C., Mortensen, J.K., and Creaser, R.A. 2004. Mid-Paleozoic initiation of the northern Cordilleran marginal backarc basin: geologic, geochemical, and neodymium isotope evidence from the oldest mafic magmatic rocks in the Yukon–Tanana terrane, Finlayson Lake district, southeast Yukon, Canada. *Geological Society of America Bulletin*, **116**: 1087–1106.
- Platt, J.P., and Vissers, R.L.M. 1989. Extensional collapse of thickened continental lithosphere: A working hypothesis for the Alboran Sea and Gibraltar Arc. *Geology*, **17**: 540–543.
- Ryan, J.J., Gordey, S.P., Villeneuve, M.E., and Piercey, S.J. 2003a. Schists and gneisses of the Yukon–Tanana terrane in the Stewart River area, western Yukon: Composition, protolith and paleotectonic setting. *In* Annual General Meeting, Vancouver, B.C. Geological Association of Canada, Vol. 28, p. A288.
- Ryan, J.J., Gordey, S.P., Glombick, P., Piercey, S.J., and Villeneuve, M.E. 2003b. Update on bedrock geological mapping of the Yukon–Tanana terrane, southern Stewart River map area, Yukon Territory. *In* Current research. Geological Survey of Canada, Vol. 2003-A9, p. 7.
- Selby, D., Creaser, R.A., and Nesbitt, B.E. 1999. Major and trace element compositions and Sr–Nd–Pb systematics of crystalline rocks from the Dawson Range, Yukon, Canada. *Canadian Journal of Earth Sciences*, **36**: 1463–1481.
- Tempelman-Kluit, D.J. 1976. The Yukon Crystalline Terrane: enigma in the Canadian Cordillera. *Geological Society of America Bulletin*, **87**: 1343–1357.
- Villeneuve, M.E., Ryan, J.J., Gordey, S.P., and Piercey, S.J. 2003. Detailed thermal and provenance history of Stewart River area (Yukon–Tanana terrane, western Yukon) through application of SHRIMP, Ar–Ar and TIMS. *In* Annual General Meeting, Vancouver, B.C. Geological Association of Canada, Vol. 28, p. A314.
- Wheeler, J.O., and McFeeley, P. 1991. Tectonic assemblage map of the Canadian Cordillera and adjacent parts of the USA. Geological Survey of Canada, Ottawa, Ont., Map 1712A, scale 1 : 2 000 000.

Appendix A

Descriptions of samples used for geochronology are based on examination by polarizing microscope, back-scattered electron images, and electron microprobe analyses.

STJBPP0012 — Metatroctolite

This rock contains fine-grained (<1 mm) olivine and plagioclase overgrown by coronae of aluminous orthopyroxene and clinopyroxene, respectively, with accessory ilmenite and biotite. The pyroxene coronae are fibrous along the grain boundaries of olivine and plagioclase but coarsen outward to grain sizes exceeding 100 µm.

STJBPP003 — Metaleucogabbro

This rock contains coarse-grained pyroxene pseudomorphed by actinolite. Calcite completely replaces plagioclase and encloses subhedral grains of primary apatite. Primary ilmenite is unaltered.

STJBPP0011 — Leucosome

Centimetre-scale layers and segregations of leucosome give this rock a heterogeneous and poorly defined gneissosity. The leucosome has granoblastic orthopyroxene (0.5–1.5 mm) and plagioclase occurring in patches that replace or overgrow biotite and that are interstitial to quartz grains. Some patches of leucosome contain euhedral garnets (<0.1 mm) with inclusion-free Ca-poor cores overgrown by Ca-rich rims. The garnet rims enclose small (<5 µm) inclusions of quartz, sillimanite, and more rarely orthopyroxene. In the leucosome, the amount of sillimanite, garnet, and orthopyroxene, and the compositions of orthopyroxene and plagioclase, vary on the scale of a thin section.